

Manganese(II) chemistry of a new N₃O-donor chelate ligand: synthesis, X-ray structures, and magnetic properties of solvent- and oxalate-bound complexes

Amy L. Fuller,^a Rex W. Watkins,^a Kim R. Dunbar,^b Andrey V. Prosvirin,^b Atta M. Arif^c and Lisa M. Berreau^{*a}

^a Department of Chemistry and Biochemistry, Utah State University, 0300 Old Main Hill, Logan, UT, 84322-0300, USA. E-mail: berreau@cc.usu.edu; Fax: +1 435-797-3390; Tel: +1 435-797-1625

^b Department of Chemistry, Texas A & M University, PO Box 30012, College Station, TX, 77842-3012, USA. E-mail: dunbar@mail.chem.tamu.edu

^c Department of Chemistry, University of Utah, 315 S. 1400 E., Salt Lake City, UT, 84112-0850, USA. E-mail: arif@chemistry.utah.edu

Received 12th January 2005, Accepted 12th April 2005
First published as an Advance Article on the web 28th April 2005

The synthesis and characterization of a new N₃O donor ligand *N*-benzyl-*N*-((6-pivaloylamido-2-pyridyl)methyl)-*N*-(2-pyridylmethyl)amine (bpppa) is reported. Treatment of bpppa with Mn(II)(ClO₄)₂·6H₂O in acetonitrile solution yielded the mononuclear [(bpppa)Mn(CH₃CN)(H₂O)](ClO₄)₂ (**1**) which was characterized by X-ray crystallography, elemental analysis, IR spectroscopy, mass spectrometry, and a solution magnetic moment measurement. Admixture of equimolar equivalents of bpppa and Mn(II)(ClO₄)₂·6H₂O in methanol solution, followed by addition of 0.5 or 1 equivalents of sodium oxalate, yielded the binuclear complex [(bpppa)Mn]₂(μ-C₂O₄)(ClO₄)₂ (**2**), which was characterized by X-ray crystallography, elemental analysis, IR spectroscopy, mass spectrometry, and solid-state magnetic measurements. While **1** is mononuclear, the formation of the binuclear oxalate derivative **2** indicates that use of the bpppa ligand does not enable isolation of a complex that is structurally relevant to a proposed 1 : 1 Mn(II)–oxalate adduct in the catalytic cycle of the oxalate degrading enzyme oxalate decarboxylase.

Introduction

Oxalic acid is biosynthesized in plants and microbes *via* enzyme-mediated reactions of oxaloacetate, glyoxylate or L-ascorbic acid.^{1–3} To regulate oxalate levels, plants and microbes have oxalate-degrading enzymes, an example of which is oxalate decarboxylase (OxdC).⁴ This enzyme catalyzes a Mn(II)/O₂-dependent carbon–carbon bond cleavage reaction that results in the conversion of oxalate to CO₂ and formate.^{4–6} The oxalate decarboxylase from *Bacillus subtilis* crystallizes as a hexamer, with each monomer unit comprising two domains.^{7,8} Each domain contains a binding site for a mononuclear Mn(II) ion. As shown in Fig. 1, the *N*-terminal domain Mn(II) center, which is believed to be the dominant or sole site of catalytic activity,⁸ is ligated in the resting state by a facial array of three histidine residues (His95, His97, His140), one glutamate (Glu101), and two water molecules, to yield an overall distorted octahedral geometry. It has been proposed that oxalate binds as a monoanion in a unidentate fashion to the Mn(II) center *via* displacement of a metal-bound water molecule (Fig. 2(a)).⁹ Reaction with O₂, coupled with displacement of the second Mn(II)-coordinated water, is proposed to yield a Mn(III) superoxide species. Deprotonation of the metal-bound oxalate is suggested to initiate decarboxylation *via* a radical pathway.⁹

To date, an X-ray crystal structure of the OxdC from *Bacillus subtilis* containing the oxalate substrate has not been reported.

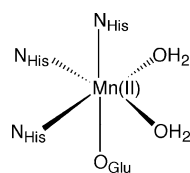


Fig. 1 Coordination environment of the active site Mn(II) center in oxalate decarboxylase (OxdC).

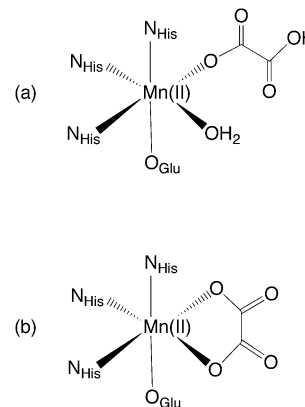


Fig. 2 Possible coordination modes of oxalate anion in OxdC.

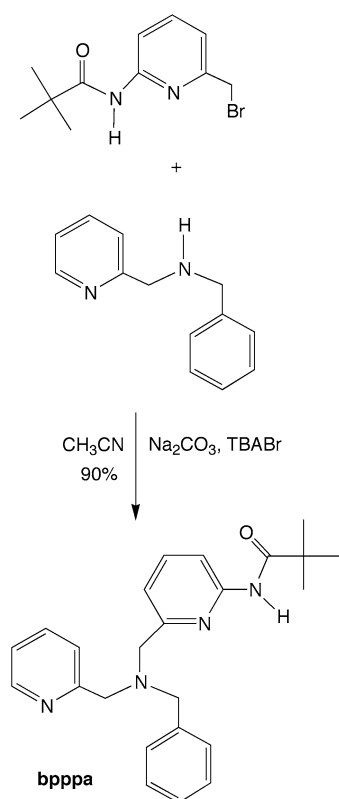
However, a recent X-ray crystallographic study of a structurally similar putative oxalate decarboxylase from *Thermotoga maritima* revealed bidentate oxalate coordination to the active site manganese ion (Fig. 2(b)).¹⁰ In the chemical literature, 1 : 1 manganese–oxalate species have been proposed to exist in aqueous solution.¹¹ A search of the Cambridge Crystallographic Database (v. 5.25, July 2004) revealed that structurally characterized examples of Mn(II) oxalate complexes, wherein four coordination positions of the Mn(II) ion are occupied by biomimetic donors akin to the amino acid ligands found in OxdC enzymes, are limited to two binuclear complexes where the oxalate dianion is coordinated in a bridging bis-bidentate type mode.¹² For Co(III) and Cr(III), use of supporting chelate amine-type ligands has enabled the isolation of mononuclear metal oxalate complexes having bidentate C₂O₄²⁻ coordination to a single metal center,^{13,14} as was found in the putative OxdC from *T. maritima*.

In this contribution, we outline studies of the manganese(II) coordination chemistry of a new N₃O-donor chelate ligand, *N*-benzyl-*N*-((6-pivaloylamido-2-pyridyl)methyl)-*N*-(2-pyridylmethyl)amine (bpppa). Using this ligand, a mononuclear six-coordinate Mn(II) complex, [(bpppa)Mn(CH₃CN)(H₂O)](ClO₄)₂ (**1**) having two *cis* coordination sites occupied by solvent molecules, has been prepared and structurally characterized. Treatment of the bpppa ligand with Mn(ClO₄)₂·6H₂O in methanol followed by addition of sodium oxalate results in the isolation of [{(bpppa)Mn}₂(μ-C₂O₄)](ClO₄)₂ (**2**), a binuclear manganese(II) complex having bis-bidentate coordination of the oxalate dianion.

Results and discussion

Synthesis of a new N₃O-donor ligand

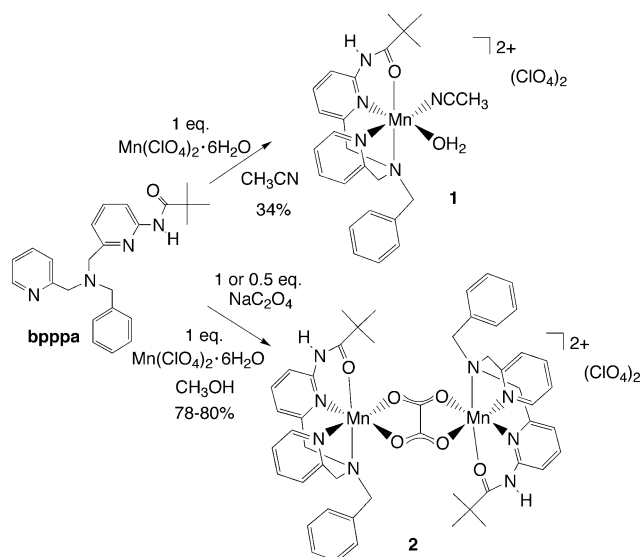
Chelate ligands containing a pyridyl donor having a 2-amido substituent have been shown to coordinate to first-row metal centers *via* the amide oxygen.¹⁵ As a first attempt toward modeling the protein-derived N₃O coordination environment of the active site manganese center in OxdC, we have constructed a new N₃O-donor ligand containing a 2-pivaloylamido moiety as the oxygen donor. Specifically, as shown in Scheme 1, treatment of 2-(pivaloylamido)-6-(bromomethyl)pyridine¹⁶ with *N*-benzyl-*N*-2-methylpyridine,¹⁷ followed by work-up and purification using silica gel column chromatography, yielded the N₃O-donor ligand *N*-benzyl-*N*-((6-pivaloylamido-2-pyridyl)methyl)-*N*-(2-pyridylmethyl)amine (bpppa) in 90% isolated yield. The bpppa ligand is a pale yellow oil that is best stored under vacuum in the freezer.



Scheme 1 Synthetic route for preparation of the bpppa ligand.

Synthesis of Mn(II) solvent- and oxalate-bound complexes

Treatment of bpppa with an equimolar amount of Mn(ClO₄)₂·6H₂O in acetonitrile, followed by recrystallization from acetonitrile–diethyl ether solution, yielded crystalline [(bpppa)Mn(CH₃CN)(H₂O)](ClO₄)₂ (**1**) in 34% isolated yield (Scheme 2). The low overall yield of crystalline complex is due to the high solubility of **1** in acetonitrile solution. Complex **1** has



Scheme 2 Synthetic routes for preparation of **1** and **2**.

been characterized by X-ray crystallography, elemental analysis, IR spectroscopy, mass spectrometry, and a solution magnetic moment measurement.

Stirring of the bpppa ligand with equimolar amounts of Mn(ClO₄)₂·6H₂O and sodium oxalate in methanol solution for several days, followed by filtration and recrystallization from CH₃CN–diethyl ether, resulted in the crystallization of only one complex, the bridging oxalate derivative [{(bpppa)Mn}₂(μ-C₂O₄)](ClO₄)₂ (**2**) in 78% yield (Scheme 2). Thus, despite providing one equivalent of oxalate dianion per manganese ion in the reaction mixture, the major product possesses a 2 : 1 manganese–oxalate stoichiometry. For reporting purposes, we have repeated the reaction using 0.5 equivalents of sodium oxalate and have obtained **2** in 80% yield. Complex **2** has been characterized by X-ray crystallography, elemental analysis, IR spectroscopy, mass spectrometry, and solid-state magnetic measurements. While complex **2** crystallizes with two non-coordinated molecules of acetonitrile (2·2CH₃CN), these solvates are lost upon drying of the bulk sample.

X-Ray crystal structures of **1** and **2**·2CH₃CN

An ORTEP representation of the cationic portion of **1** is shown in Fig. 3. Details of the data collection and refinement are given

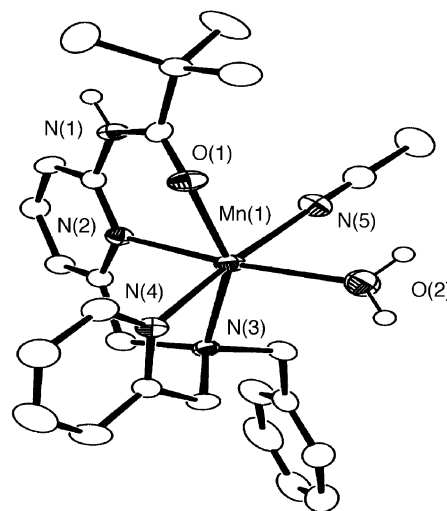


Fig. 3 ORTEP drawing of the cationic portion of **1**. Ellipsoids are plotted at the 50% probability level. All hydrogen atoms, except those on the amide and manganese-coordinated water molecule, have been omitted for clarity.

Table 1 Summary of X-ray data collection and refinement

	1	2·2CH₃CN
Empirical formula	C ₂₆ H ₃₃ N ₅ Cl ₂ O ₁₀ Mn	C ₅₀ H ₅₆ N ₈ Cl ₂ O ₁₄ Mn ₂ ·(CH ₃ CN) ₂
<i>M_r</i>	701.41	1255.92
Crystal system	Orthorhombic	Triclinic
Space group	<i>Pna</i> 2 ₁	<i>P</i> $\bar{1}$
<i>a</i> /Å	32.1996(8)	14.5730(2)
<i>b</i> /Å	9.2019(2)	14.6144(2)
<i>c</i> /Å	10.5751(2)	16.9418(2)
<i>a</i> /°	90	71.2141(9)
<i>β</i> /°	90	66.7123(9)
<i>γ</i> /°	90	63.7564(8)
<i>V</i> /Å ³	3133.38(12)	2924.77(7)
<i>Z</i>	4	2
<i>D_c</i> /Mg m ⁻³	1.487	1.426
<i>T</i> /K	150(1)	150(1)
Color	Colorless	Colorless
Crystal habit	Prism	Prism
Crystal size/mm ³	0.30 × 0.25 × 0.23	0.30 × 0.23 × 0.20
Diffractometer	Nonius KappaCCD	Nonius KappaCCD
<i>μ</i> /mm ⁻¹	0.653	0.595
2 θ _{max} /°	54.96	54.96
Completeness to $\theta = 27.48^\circ$ (%)	99.4	99.6
Reflections collected	6699	23355
Independent reflections	6699	13322
<i>R</i> _{int}	—	0.0206
Variable parameters	424	1004
<i>R</i> 1/ <i>wR</i> 2 ^b	0.0425/0.0984	0.0518/0.1216
Goodness-of-fit (<i>F</i> ²)	1.020	1.017
$\Delta\rho_{\max/\min}$ /e Å ⁻³	0.514/−0.418	1.048/−0.929

^a Radiation used: Mo-K α ($\lambda = 0.71073$ Å). ^b $R1 = \sum||F_o| - |F_c|| / \sum|F_o|$; $wR2 = [\sum[w(F_o^2 - F_c^2)^2] / \sum(F_o^2)]^{1/2}$ where $w = 1/[\sigma^2(F_o^2) + (aP)^2 + bP]$.

in Table 1. Selected bond distances and angles are given in Table 2. The overall geometry of the Mn(II) ion in **1** is distorted octahedral, with a notable feature being the O(1)–Mn(1)–N(3) angle (154.03(9)°), which is significantly below 180° due to the chelate nature of the bpppa ligand. This angle is acute relative to the largest N_{HIS}–Mn–O_{Glu} angle in the active site Mn(II) center of OxdC (173°).⁸ However, similar to the enzyme active site Mn(II) center in OxdC, **1** exhibits N₃O-coordination of the chelate ligand and two *cis* solvent-occupied coordination sites. The three nitrogen donors of the bpppa ligand form a facial

array on the metal center akin to the three histidine donors found in OxdC, albeit the average of the N–Mn–N bond angles in **1** (84°) is smaller than the average of the N_{HIS}–Mn–N_{HIS} bond angles in OxdC (94°), again due to the chelate nature of the bpppa ligand.⁸ The average Mn–N distance for the bpppa nitrogen donor atoms in **1** (2.24 Å) is similar to the average Mn–N_{HIS} distance (2.27 Å) in the enzyme.⁸ In addition, the Mn(1)–O(1) interaction in **1** (2.089(2) Å) is generally similar to the N-terminal Mn(II)–O_{Glu} interaction (2.04 Å). However, the metal–water interaction in **1** (Mn(1)–O(2) 2.136(2) Å) is

Table 2 Selected bond lengths (Å) and angles (°) for **1** and 2·2CH₃CN^a

[(bpppa)Mn(H ₂ O)(CH ₃ CN)](ClO ₄) ₂ (1)		[{(bpppa)Mn} ₂ (μ-C ₂ O ₄)](ClO ₄) ₂ ·2CH ₃ CN (2·2CH₃CN)			
Mn(1)–O(1)	2.089(2)	Mn(1)–O(2)	2.1150(18)	Mn(2)–O(1)	2.116(2)
Mn(1)–O(2)	2.136(2)	Mn(1)–O(5)	2.1689(17)	Mn(2)–O(3)	2.1378(17)
Mn(1)–N(5)	2.290(3)	Mn(1)–O(6)	2.1611(17)	Mn(2)–O(4)	2.1967(18)
Mn(1)–N(2)	2.229(3)	Mn(1)–N(6)	2.272(2)	Mn(2)–N(2)	2.249(2)
Mn(1)–N(3)	2.270(2)	Mn(1)–N(7)	2.282(2)	Mn(2)–N(3)	2.298(2)
Mn(1)–N(4)	2.215(3)	Mn(1)–N(8)	2.240(2)	Mn(2)–N(4)	2.254(2)
O(1)–Mn(1)–O(2)	102.17(11)	O(2)–Mn(1)–O(5)	97.16(7)	O(1)–Mn(2)–O(3)	90.85(7)
O(1)–Mn(1)–N(2)	81.25(9)	O(2)–Mn(1)–O(6)	108.95(7)	O(1)–Mn(2)–O(4)	128.17(8)
O(1)–Mn(1)–N(3)	154.03(9)	O(2)–Mn(1)–N(6)	79.96(7)	O(1)–Mn(2)–N(2)	80.24(8)
O(1)–Mn(1)–N(4)	93.46(9)	O(2)–Mn(1)–N(7)	104.96(7)	O(1)–Mn(2)–N(3)	139.95(8)
O(1)–Mn(1)–N(5)	89.47(9)	O(2)–Mn(1)–N(8)	89.27(8)	O(1)–Mn(2)–N(4)	86.56(10)
O(2)–Mn(1)–N(2)	166.99(11)	O(5)–Mn(1)–O(6)	76.60(6)	O(3)–Mn(2)–O(4)	76.38(6)
O(2)–Mn(1)–N(3)	101.85(10)	O(5)–Mn(1)–N(6)	164.47(7)	O(3)–Mn(2)–N(2)	156.93(7)
O(2)–Mn(1)–N(4)	93.18(10)	O(5)–Mn(1)–N(7)	115.29(7)	O(3)–Mn(2)–N(3)	123.26(8)
O(2)–Mn(1)–N(5)	83.18(10)	O(5)–Mn(1)–N(8)	83.48(7)	O(3)–Mn(2)–N(4)	91.83(8)
N(2)–Mn(1)–N(3)	77.53(8)	O(6)–Mn(1)–N(6)	89.83(7)	O(4)–Mn(2)–N(2)	92.41(7)
N(2)–Mn(1)–N(4)	99.17(10)	O(6)–Mn(1)–N(7)	99.65(7)	O(4)–Mn(2)–N(3)	83.84(7)
N(2)–Mn(1)–N(5)	84.31(10)	O(6)–Mn(1)–N(8)	154.34(8)	O(4)–Mn(2)–N(4)	142.68(9)
N(3)–Mn(1)–N(4)	75.49(10)	N(6)–Mn(1)–N(7)	73.99(7)	N(2)–Mn(2)–N(3)	74.35(8)
N(3)–Mn(1)–N(5)	103.04(10)	N(6)–Mn(1)–N(8)	111.60(8)	N(2)–Mn(2)–N(4)	108.66(8)
N(4)–Mn(1)–N(5)	175.75(10)	N(7)–Mn(1)–N(8)	74.34(7)	N(3)–Mn(2)–N(4)	73.25(9)

^a Estimated standard deviations indicated in parentheses.

shorter than that found at the active site Mn(II) center in OxdC (av. Mn(II)–O(H₂O) 2.35 Å).⁸ This is likely due to a reduced Lewis acidity for the enzyme N₃O(glutamate)-ligated Mn(II) center. Thus, while the bpppa ligand provides a N₃O donor environment for the Mn(II) ion in which the chelate ligand–Mn(II) bond distances are similar to those found for Mn(II)–protein interactions in OxdC, the bpppa ligand does not accurately reproduce the primary ligand environment of the enzyme Mn(II) center in terms of bond angles and charge. Finally, both protons of the Mn(II)-bound water molecule of **1** are involved in moderate hydrogen-bonding interactions with a perchlorate anion in the solid state (O(2)···O(7)/O(8) 2.75/2.73 Å; O(2)–H···O(7)/O(8) 168/165°).¹⁸ A moderate hydrogen bonding interaction is defined as having a heteroatom distance (A···B) of 2.5–3.2 Å, a A–H···B angle of 130–180°, and energy of 4–15 kcal mol⁻¹.¹⁸

ORTEP representations of the (a) binuclear cationic portion, and (b) Mn₂(μ-C₂O₄) core of 2·2CH₃CN are shown in Fig. 4. As in **1**, the bpppa ligand is bound to each Mn(II) center of the binuclear cation in a tetradentate fashion with each metal center having a distorted octahedral geometry. The oxalate dianion is bound between the two Mn(II) ions of 2·2CH₃CN in a bis-bidentate fashion. This structural motif has been previously identified in two Mn(II) complexes having N₄-donor tetradentate supporting chelate ligands.¹² The Mn(1)···Mn(2) separation (5.62 Å) and oxalate C–O and C–C bond lengths in 2·2CH₃CN are identical to those found in [(bispicMe₂en)Mn(C₂O₄)Mn(bispicMe₂en)](ClO₄)₂.¹² However, one distinct feature of 2·2CH₃CN is a slight asymmetry for the oxalate anion binding to Mn(2). Specif-

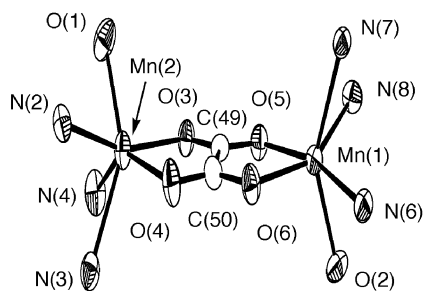
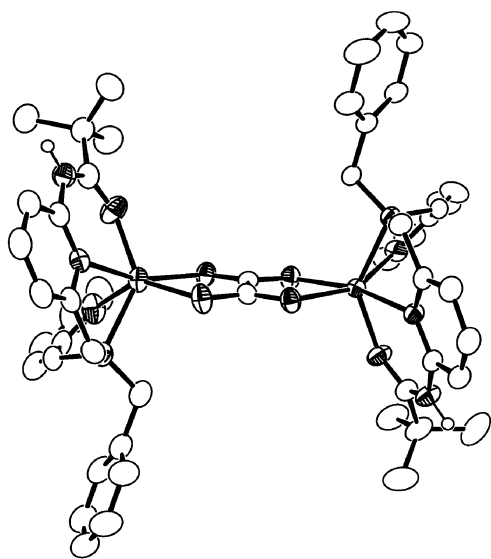


Fig. 4 ORTEP representations of the cationic portion (top) and Mn(II) coordination environments (bottom) in 2·2CH₃CN. Ellipsoids are plotted at the 50% probability level. All hydrogen atoms, except the proton on the amide moiety, have been omitted for clarity.

ically, the Mn(2)–O(3) bond is ~0.06 Å shorter than the Mn(2)–O(4) interaction. This contrasts with identical Mn–O bond lengths for the Mn(1) ion of 2·2CH₃CN (Mn(1)–O(5) 2.1689(17), Mn(1)–O(6) 2.1611(17) Å) and both manganese centers in [(bispicMe₂en)Mn(C₂O₄)Mn(bispicMe₂en)](ClO₄)₂ (Mn–O 2.160(3) and 2.168(3) Å).¹² Finally, the Mn–N and Mn–O distances involving the bpppa chelate ligands in 2·2CH₃CN are slightly longer than those found in **1**, consistent with reduced Lewis acidity of the Mn(II) centers in the binuclear complex due to oxalate dianion coordination.

Magnetic properties of **1** and **2**

The solution magnetic moment of **1** was determined at 298 K using the Evans method.¹⁹ The mononuclear Mn(II) complex **1** exhibits $\mu_{\text{eff}} = 5.8 \mu_{\text{B}}$, consistent with the expected spin-only value ($5.9 \mu_{\text{B}}$) for a mononuclear high-spin Mn(II) center ($S = 5/2$). Solid-state magnetic susceptibility measurements of **2** were performed on a polycrystalline sample of **2** at 1000 Oe over the temperature range 2–300 K. A plot of the χT vs. T susceptibility data for **2** is shown in Fig. 5. The value of χT at 300 K is 8.32 emu mol⁻¹ K, which is slightly lower than the expected spin-only value for two Mn(II) ions ($2\chi_{(S=5/2)}T = 8.75$ emu mol⁻¹ K). As the temperature is lowered, the χT value decreases gradually to 0.36 emu mol⁻¹ K at 2 K. The temperature dependence of $1/\chi$ in the temperature range 7–300 K approximates Curie–Weiss behavior with $C = 9$ emu mol⁻¹ K and $\theta = -20$ K. The negative Curie–Weiss constant indicates that the coupling between the Mn(II) centers is antiferromagnetic.²⁰ The weak antiferromagnetic coupling observed for **2** is similar to that found for binuclear Mn(II) oxalate complexes of the tetradentate N₄-donor ligands *N,N'*-bis(2-pyridylmethyl)-1,2-ethanediamine, *N,N'*-bis(2-pyridylmethyl)-1,3-propanediamine, and *N,N'*-bis(2-pyridylmethyl)-*N,N'*-dimethyl-1,2-ethanediamine. In this set of complexes, the effective magnetic moment at ambient temperature is 8.3–8.4 μ_{B} .¹²

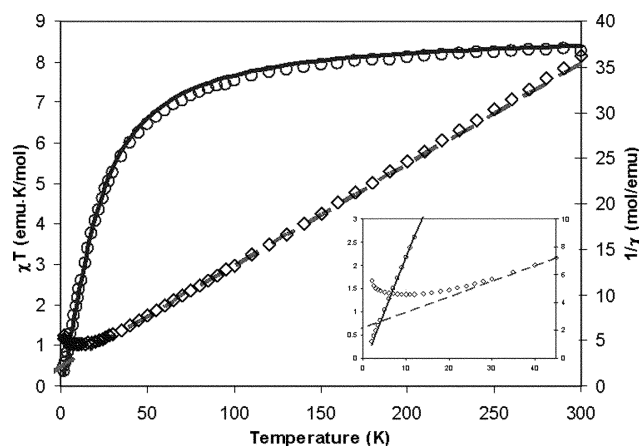


Fig. 5 Temperature dependence of the χT product (○) and the inverse susceptibility (◇) for **2**. The solid line corresponds to the best fit obtained with eqn. (2), and the dashed line corresponds to the best fit to the Curie–Weiss law. The inset shows the deviation from Curie–Weiss behavior at low temperature.

In the solid state, **2** contains two $S = 5/2$ Mn(II) centers bridged by an oxalate ligand which is expected to lead to dominant intramolecular exchange interactions. Accordingly, the variable-temperature magnetic susceptibility data for this complex were fit to the modified Van Vleck equation (eqn. (1)) using the isotropic exchange Hamiltonian ($H = -JS_1 \cdot S_2 + g\mu_{\text{B}}S_z H - zJ'(S_z)_i(S_z)_j$) for two interacting $S = 5/2$ centers with $x = J/kT$.²⁰ In an effort to include intermolecular interactions between individual binuclear molecules, the expression in eqn. (1) was corrected using the molecular field approximation (eqn. (2)) where χ is the exchange coupled magnetic susceptibility that was measured, χ_{dim} is the magnetic susceptibility of the Mn dimer, zJ'

is the exchange parameter and the other symbols have their usual meanings. The magnetic data can be fit very well to eqn. (2) in the temperature range of 2–300 K (Fig. 6) with $J = -2.95 \text{ cm}^{-1}$, $g = 2.0$ and $zJ' \approx 0 \text{ cm}^{-1}$. The fact that zJ' is essentially zero means that intermolecular interactions are negligible and can be ignored.

$$\chi_{\text{dim}} = \frac{2Ng^2\beta^2}{kT} \frac{e^x + 5e^{3x} + 14e^{6x} + 30e^{10x} + 55e^{15x}}{1 + 3e^x + 5e^{3x} + 7e^{6x} + 9e^{10x} + 11e^{15x}} \quad (1)$$

$$\chi = \frac{\chi_{\text{dim}}}{1 - (zJ'/Ng^2\beta^2)\chi_{\text{dim}}} \quad (2)$$

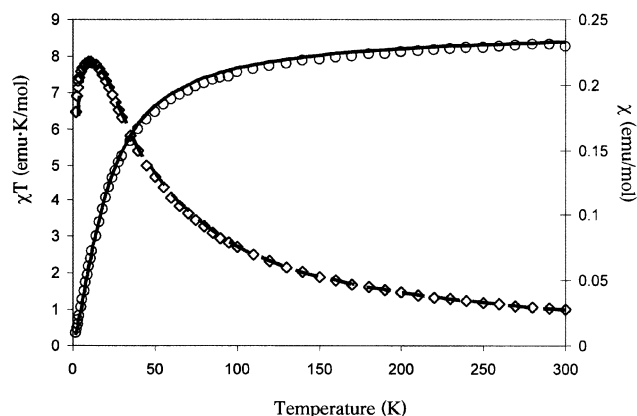


Fig. 6 Temperature dependence of the χT product (○) and the molar susceptibility (◇). The solid and dashed lines correspond to the best fit obtained with eqn. (2).

Conclusion

Recent X-ray crystallographic and mechanistic studies of Mn(II)-containing oxalate decarboxylase (OxdC) suggest that the catalytic pathway for this enzyme involves reaction of a N_3O -ligated Mn(II)-oxalate adduct with O_2 to yield carbon dioxide and formate.^{7–9} While the structural features of the Mn(II)-oxalate species in OxdC remain unknown, both mono- and bidentate coordination modes have been observed in first-row transition-metal complexes and may be possible in the enzyme active site.^{8,10} In the work presented herein, we have evaluated whether use of the new N_3O -donor bpppa chelate ligand would enable the isolation of synthetic complexes with relevance to species proposed in the catalytic cycle of OxdC. While **1** is mononuclear and supported by a N_3O -donor ligand environment, isolation of the binuclear oxalate derivative **2**, which has structural and magnetic properties similar to previously reported complexes supported by N_4 -donor chelate ligands,¹² indicates that the bpppa ligand is not suitable for the isolation of a mononuclear Mn(II) oxalate derivative relevant to an enzyme/substrate adduct. On the basis of these data, efforts are underway to incorporate steric hindrance and/or hydrogen-bond donors into a supporting N_3O -donor chelate ligand, with the goal of preventing the formation of binuclear oxalate derivatives. In this regard, it is worth noting that a proposed structure for the enzyme/substrate adduct in OxdC includes hydrogen-bonding interactions between the Mn(II)-bound oxalate and surrounding amino acid residues.⁸

Experimental

General

All chemicals were purchased from commercial sources and used as received unless otherwise noted. All reactions involving Mn(II) salts were performed in a MBraun Unilab glovebox under an atmosphere of purified dinitrogen. Solvents for glovebox procedures were dried according to published methods and

distilled under N_2 prior to use.²¹ ^1H and ^{13}C NMR were obtained in CD_3CN solution on a Bruker ARX-400 spectrometer at 25(1) °C. Chemical shifts are reported relative to the residual solvent signals (^1H NMR: CHD_2CN , δ 1.94 (quintet); $^{13}\text{C}\{^1\text{H}\}$ NMR: δ 1.39 (heptet)). FTIR spectra were recorded on a Shimadzu FTIR-8400 spectrometer as KBr pellets. Room-temperature magnetic susceptibilities were determined by the Evans method.¹⁹ Mass spectrometry data was obtained at the Mass Spectrometry Facility, Department of Chemistry, University of California, Riverside. Elemental analyses were performed by Atlantic Microlabs, Inc., Norcross, Georgia. Variable temperature magnetic susceptibility data for **2** were collected using a solid microcrystalline sample on a Quantum Design MPMS-2 SQUID magnetometer in the range of 2–300 K.

The ligand precursors 2-(pivaloylamido)-6-(bromomethyl)-pyridine and *N*-benzyl-*N*-2-methylpyridine were prepared according to literature procedures.^{16,17}

Synthesis of ligand and complexes

***N*-Benzyl-*N*-((6-pivaloylamido-2-pyridyl)methyl)-*N*-(2-pyridylmethyl)amine (bpppa).** To a 500 mL round bottom flask containing 2-(pivaloylamido)-6-(bromomethyl)pyridine (2.1 g, 7.5 mmol, 50 mL) in dry acetonitrile (70 mL) was added *N*-benzyl-*N*-2-methylpyridine (1.5 g, 7.5 mmol, 20 mL), Na_2CO_3 (1.6 g, 15 mmol), and a catalytic amount of tetrabutylammonium bromide (~5 mg). The reaction mixture was purged with nitrogen and refluxed for 22 h. After cooling the solution to room temperature, 1 M sodium hydroxide was added (90 mL). The resulting biphasic solution was extracted with dichloromethane ($3 \times 150 \text{ mL}$) and the organic fractions were combined and dried over anhydrous sodium sulfate. After filtration, the organic solution was brought to dryness under reduced pressure. Column chromatography on silica gel (230–400 mesh; ethyl acetate, $R_f = 0.55$), followed by removal of the solvent under reduced pressure, yielded a yellow oil (2.63 g, 90%) (Found: C, 74.03; H, 7.25; N, 14.32. $\text{C}_{24}\text{H}_{28}\text{N}_4\text{O}$ requires C, 74.18; H, 7.27; N, 14.43%; $\nu_{\text{max}}/\text{cm}^{-1}$: (N–H) 3350 (br), (C=O) 1687 (neat); δ_{H} (400 MHz, solvent CD_3CN): 1.26 (9H, s), 3.65 (2H, s), 3.66 (2H, s), 3.75 (2H, s), 7.15–7.27 (2H, m), 7.30–7.36 (3H, m), 7.42 (2H, d, $J = 7.4 \text{ Hz}$), 7.57 (1H, d, $J = 7.8 \text{ Hz}$), 7.69 (2H, t, $J = 7.8 \text{ Hz}$), 7.98 (1H, d, $J = 8.2 \text{ Hz}$), 8.14 (1H, br s, N–H), 8.46 (1H, d, $J = 4.5 \text{ Hz}$); δ_{C} (100 MHz, CD_3CN): 27.7, 40.5, 59.1, 60.3, 60.7, 112.7, 119.4, 123.1, 123.9, 128.1, 129.3, 130.0, 137.4, 139.6, 140.4, 149.9, 152.3, 159.5, 160.8, 178.0 (20 signals expected and observed); FAB-MS: m/z 389 (MH^+ , 100%).

CAUTION! Perchlorate complexes of organic ligands are potentially explosive. They should be handled in small quantities with great care.²²

[(bpppa)Mn(CH₃CN)(H₂O)](ClO₄)₂ (1**).** To a acetonitrile (3 mL) solution of bpppa (0.054 g, 0.14 mmol) was added a acetonitrile (3 mL) solution of $\text{Mn}(\text{ClO}_4)_2 \cdot 6\text{H}_2\text{O}$ (0.050 g, 0.14 mmol). The resulting yellow solution was stirred for ~3 h at ambient temperature. The solvent was then removed under reduced pressure. The remaining solid was dissolved in ~4 mL of acetonitrile and diethyl ether (~10 mL) was added until the solution became cloudy. From this solution, block-type colorless crystals were obtained (0.033 mg, 34%) (Found C, 44.55 H, 4.78 N, 9.88. $\text{C}_{26}\text{H}_{33}\text{N}_5\text{O}_{10}\text{ClMn}$ requires C, 44.57; H, 4.75; N, 10.00%; $\nu_{\text{max}}/\text{cm}^{-1}$: 3386s, 3319s, 1654s, 1619s, 1528m, 1459s, 1438m, 1420m, 1162m, 1112s, 1066s, 623s (KBr); FAB-MS (DCM–NBA), m/z (relative intensity): 542 ($[\text{M} + \text{ClO}_4]^-$, 32%); $\mu_{\text{eff}}(\text{CH}_3\text{CN}, 25(1) \text{ }^\circ\text{C}) = 5.8 \mu_{\text{B}}$.

[(bpppa)Mn]₂(μ -C₂O₄)](ClO₄)₂ (2**).** To a methanol solution (3 mL) of bpppa (0.052 g, 0.13 mmol) was added a methanol solution (3 mL) of $\text{Mn}(\text{ClO}_4)_2 \cdot 6\text{H}_2\text{O}$ (0.048 g, 0.13 mmol).

The resulting pale yellow solution was stirred for ~20 min at ambient temperature. This solution was added to Na₂C₂O₄ (0.009 g, 0.07 mmol) and the reaction mixture was stirred for six days at which point the solvent was removed under reduced pressure. The solid was re-dissolved in methylene chloride and filtered through a glass wool/Celite plug. The CH₂Cl₂ solvent was removed from the filtrate under reduced pressure leaving a white solid. Recrystallization of the solid from CH₃CN–diethyl ether at –20(1) °C yielded colorless crystalline blocks (0.062 g, 80%) (Found: C, 50.84; H, 4.85; N, 9.54. C₅₀H₅₆N₈O₁₄Cl₂Mn₂ requires C, 51.19; H, 4.81; N, 9.56%; ν_{\max} /cm⁻¹ 1664s, 1641s, 1614s, 1524s, 1483m, 1458s, 1310m, 1163m, 1096s, 1016m, 793m, 770m, 752m, 706m, 623s; FAB-MS (DCM–NBA), *m/z* (relative intensity): 1073 ([M – ClO₄]⁺, 15%).

X-Ray crystallography

A crystal of each manganese complex was mounted on a glass fiber using a viscous oil and then transferred to a Nonius KappaCCD diffractometer with Mo-K α radiation (λ = 0.71073 Å) for data collection at 150(1) K. For each compound, an initial set of cell constants was obtained from 10 frames of data that were collected with an oscillation range of 1° frame⁻¹ and an exposure time of 20 s frame⁻¹. Indexing and unit cell refinement based on all observed reflections from those 10 frames indicated an orthorhombic *P* lattice for **1** and a triclinic *P* lattice for **2·2CH₃CN**. Final cell constants for each complex were determined from a set of strong reflections from the actual data collection. For each data set, reflections were indexed, integrated, and corrected for Lorentz, polarization, and absorption effects using DENZO-SMN and SCALEPAC.²³ The structures of **1** and **2·2CH₃CN** were solved using a combination of direct methods and heavy atom methods using SIR 97.²⁴

For **1**, all of the non-hydrogen atoms except for the oxygen atoms of one perchlorate anion were refined with anisotropic displacement coefficients. The hydrogen atoms on the coordinated water molecule and the amide proton in **1** were located and refined independently. All other hydrogen atoms for **1** were assigned isotropic displacement coefficients $U(\text{H}) = 1.2U(\text{C})$ or $1.5U(\text{C}_{\text{methyl}})$, and their coordinates were allowed to ride on their respective carbons using SHELXL97.²⁵ There is one disordered perchlorate anion in **1**. The O(7), O(8) and O(9) oxygen atoms, bonded to Cl(2), were each split into two fragments (O(7)/O(7'), O(8)/O(8'), O(9)/O(9')) and were refined. This refinement led to a 0.87 : 0.13 ratio in occupancy over two positions for O(7) and O(8) and a 0.60 : 0.40 ratio in occupancy over two positions for O(9). The O(10) atom was split into three fragments (O(10)/O(10')/O(10'')), with refinement leading to a 0.55 : 0.27 : 0.18 ratio in occupancy over three positions.

For **2·2CH₃CN**, all of the non-hydrogen atoms, except select oxygen atoms of the perchlorate anions, were refined with anisotropic displacement coefficients. All hydrogen atoms, except those of two non-coordinated acetonitrile solvate molecules, were located and refined independently. The solvate hydrogen atoms of **2·2CH₃CN** were assigned isotropic displacement coefficients $U(\text{H}) = 1.2U(\text{C})$ or $1.5U(\text{C}_{\text{methyl}})$, and their coordinates were allowed to ride on their respective carbons using SHELXL97.²⁵ The position of the methyl carbon of one acetonitrile solvate molecule is disordered over two positions. Splitting of C(54) into two fragments (C(54)/C(54')) and refinement led to a 0.54 : 0.46 ratio in occupancy. Oxygen atoms of both perchlorate anions in **2·2CH₃CN** exhibit disorder.

CCDC reference numbers 259639 and 259640.

See <http://www.rsc.org/suppdata/dt/b5/b500534e/> for crystallographic data in CIF or other electronic format.

Acknowledgements

L. M. B. gratefully acknowledges the Herman Frasch Foundation (501-HF02) for financial support. K. R. D. gratefully acknowledges the National Science Foundation (DMR0103455, NSF-9974899) and the Telecommunication and Informatics Task Force (TITF) at Texas A & M University. The SQUID magnetometer was purchased with funds provided by the National Science Foundation.

References

- 1 A. Hodgkinson, *Oxalic Acid in Biology and Medicine*, Academic Press, London, 1977.
- 2 S. R. Kahn, *Calcium Oxalate in Biological Systems*, CRC Press, Boca Raton, FL, 1995.
- 3 S. E. Keates, N. M. Tarlyn, F. A. Loewus and V. R. Franceschi, *Phytochemistry*, 2000, **53**, 433.
- 4 M. V. Dutton and C. S. Evans, *Can. J. Microbiol.*, 1996, **42**, 881.
- 5 A. Tanner and S. Bornemann, *J. Bacteriol.*, 2000, **182**, 5271.
- 6 A. Tanner, L. Bowater, S. A. Fairhurst and S. Bornemann, *J. Biol. Chem.*, 2001, **276**, 43627.
- 7 R. Anand, P. C. Dorresteijn, C. Kinsland, T. P. Begley and S. E. Ealick, *Biochemistry*, 2002, **41**, 7659.
- 8 V. J. Just, C. E. M. Stevenson, L. Bowater, A. Tanner, D. M. Lawson and S. Bornemann, *J. Biol. Chem.*, 2004, **279**, 19867.
- 9 L. A. Reinhardt, D. Svedruzic, C. H. Chang, W. W. Cleland and N. G. J. Richards, *J. Am. Chem. Soc.*, 2003, **125**, 1244.
- 10 R. Schwarzenbacher, F. von Delft, L. Jaroszewski, P. Abdubek, E. Ambing, T. Biorac, L. S. Brinen, J. M. Canaves, J. Cambell, H.-J. Chiu, X. Dai, A. M. Deacon, M. DiDonato, M.-A. Elsliger, S. Eshagi, R. Floyd, A. Godzik, C. Grittini, S. K. Grzechnik, E. Hampton, C. Karlak, H. E. Klock, E. Koesema, J. S. Kovarik, A. Kreuzsch, P. Kuhn, S. A. Lesley, I. Levin, D. McMullan, T. M. McPhillips, M. D. Miller, A. Morse, K. Moy, J. Ouyang, R. Page, K. Quijano, A. Robb, G. Spraggon, R. C. Stevens, H. van den Bedem, J. Velasquez, J. Vincent, X. Wang, B. West, G. Wolf, Q. Xu, K. O. Hodgson, J. Wooley and I. A. Wilson, *Proteins*, 2004, **56**, 392.
- 11 B. Chiswell, E. D. McKenzie and L. F. Lindoy, *Comprehensive Coordination Chemistry*, Pergamon, New York, 1987, vol. 4, pp. 1–122.
- 12 J. Glerup, P. A. Goodson, D. J. Hodgson and K. Michelsen, *Inorg. Chem.*, 1995, **34**, 6255.
- 13 S. Yano, S. Yaba, M. Ajioka and S. Yoshikawa, *Inorg. Chem.*, 1979, **18**, 2414.
- 14 J. W. Lethbridge, L. S. D. Glasser and H. F. W. Taylor, *J. Chem. Soc. A*, 1970, 1862.
- 15 See for example: L. M. Berreau, M. M. Makowska-Grzyska and A. M. Arif, *Inorg. Chem.*, 2000, **39**, 4390.
- 16 L. M. Berreau, S. Mahapatra, J. A. Halfen, V. G. Young, Jr. and W. B. Tolman, *Inorg. Chem.*, 1996, **35**, 6339.
- 17 D. J. E. Spencer, B. J. Johnson, B. J. Johnson and W. B. Tolman, *Org. Lett.*, 2002, **4**, 1391.
- 18 G. A. Jeffrey, *An Introduction to Hydrogen Bonding*, Oxford University Press, New York, 1997.
- 19 D. F. Evans, *J. Chem. Soc.*, 1959, 2003.
- 20 O. Kahn, *Molecular Magnetism*, VCH Publishers, New York, 1993.
- 21 W. L. F. Armarego, D. D. Perrin, *Purification of Laboratory Chemicals*, Butterworth-Heinemann, Boston, MA, 4th edn., 1996.
- 22 W. C. Wolsey, *J. Chem. Educ.*, 1973, **50**, A335.
- 23 Z. Otwinowski and W. Minor, *Methods Enzymol.*, 1997, **276**, 307.
- 24 A. Altomare, M. C. Burla, M. Camalli, G. L. Casciarano, C. Giacovazzo, A. Guagliardi, A. G. G. Moliterni, G. Polidori and R. Spagna, *J. Appl. Crystallogr.*, 1999, **32**, 115.
- 25 G. M. Sheldrick, *SHELXL-97, Program for the Refinement of Crystal Structures*, University of Göttingen, 1997.